01 Sep 2011

Earthquake-Induced Deformation Analysis of a Bridge Approach Embankment in Missouri

W. Liu

Ronaldo Luna
Missouri University of Science and Technology, rluna@mst.edu

Richard Wesley Stephenson
Missouri University of Science and Technology, rwstephenson@mst.edu

S. Wang

Recommended Citation

W. Liu et al., "Earthquake-Induced Deformation Analysis of a Bridge Approach Embankment in Missouri," *Geotechnical and Geological Engineering*, vol. 29, no. 5, pp. 845 - 854, Springer, Sep 2011.
The definitive version is available at https://doi.org/10.1007/s10706-011-9421-1

Geotech Geol Eng (2011) 29:845–854
DOI 10.1007/s10706-011-9421-1

ORIGINAL PAPER

Earthquake-Induced Deformation Analysis of a Bridge Approach Embankment in Missouri

W. Liu · R. Luna · R. W. Stephenson · S. Wang

Received: 24 September 2009 / Accepted: 3 June 2011 / Published online: 17 June 2011

Abstract Earthquake-induced deformations for a bridge approach earth embankment are predicted using a calibrated numerical model. The constitutive soil model is a modified hyperbolic model that uses Masing rules and incremental pore pressure relations. The model was calibrated using both laboratory and field data. A shaking table physical model was used to verify the numerical simulation. Additionally, the upper San Fernando dam was modeled to reproduce the deformations in the 1971 earthquake. The subsurface and embankment soil conditions were characterized using field and laboratory methods. The model developed was used to predict the earthquake-induced deformations of an approach embankment to Bridge A1466 in the NMSZ near Hayti, Missouri, where strong earthquakes $M > 7.0$ are anticipated in the next 50 years.

Keywords Bridge approach embankment · Seismic deformations · Nonlinear model · Finite element · Shaking table

W. Liu
Parsons Brinkerhoff, Lawrenceville, NJ 08648, USA

R. Luna (✉) · R. W. Stephenson · S. Wang
Missouri University of Science and Technology, Rolla, MO 65409, USA
e-mail: rluna@mst.edu

1 Introduction

Quantifying earthquake-induced deformations is one of the biggest challenges in geotechnical earthquake engineering, especially when the foundation soils may liquefy. There are a number of methods to analyze the seismic stability of slopes that include both limit equilibrium and deformation analysis, but the deformations during earthquakes are more difficult to calculate. Newmark (1965) first modeled the soil displacement under cyclic loading as a rigid block translating on an inclined plane. Makdisi and Seed (1978) extended Newmark's approach to include the structural response of moderately high embankments. Rathje and Bray (1999) and Lin and Hynes (1998) reviewed the Newmark type of deformation analysis.

More complicated numerical analysis approaches use different nonlinear soil models have been proposed and applied in different software applications. Finn et al. (1986) used a nonlinear hysteretic stress–strain soil model in the finite element program TARA-3. The Martin–Finn-Seed approach (Martin et al. 1975) was combined into a nonlinear hyperbolic stress–strain soil model to calculate pore pressure and liquefaction by Finn et al. (1999). Wu (1998, 2001) modified the unloading–reloading modulus in the MFS model and developed a numerical analysis program entitled VERSAT. Some elasto-plastic models using Biot's coupled equations were developed for pore pressure and deformation calculations. The

representative codes are DYNAFLOW (Prevost 1981), DYSAC2 (Muraleetharan et al. 1988), and SWANDYNE4 (Zienkiewicz et al. 1990a, b).

The Finn model is available in the FLAC software package as a built-in feature. This model does not consider the following: shear modulus degradation, damping, shear strength variation, and variations of the maximum shear modulus due to changes in effective confining pressure. In this study, a hyperbolic model was modified and calibrated against both a shaking table test and the 1971 failure of Upper San Fernando Dam before it was implemented to predict the seismic performance of a bridge approach embankment in Missouri's New Madrid Seismic Zone (NMSZ).

2 Modified Hyperbolic Model

The two-dimensional finite difference computer program FLAC was used including two different constitutive models. One was the built-in "Finn model" which combines the Mohr–Coulomb and Martin et al. (1975) and Byrne (1991) models. The other model used was the modified hyperbolic model combined with the Martin/Byrne model and implemented into FLAC. The modified hyperbolic model is presented herein.

The model was based on two of Masing's rules for the behavior of soil under dynamic loading. Two generalized functional forms were developed, including the Davidenkov-class and Ramberg–Osgood-class models (Masing 1926). The former gives the shear stress in terms of the shear strain, and the latter gives the shear strain in terms of the shear stress. A hyperbola can be expressed in either the Davidenkov form or the Ramberg–Osgood form.For initial loading, the stress–strain curve follows the backbone function.

$$\tau = \frac{G_{\max}\gamma}{1 + \left|\frac{\gamma}{\gamma_r}\right|} \tag{1}$$

For reloading and unloading, the stress–strain curve follows path given by

$$\tau = \tau_c + \frac{G_{\max}(\gamma - \gamma_c)}{1 + \left|\frac{\gamma - \gamma_c}{2\gamma_r}\right|} \tag{2}$$

where $\tau_{\max}$ and γ_r ($\gamma_r = \tau_{\max}/G_{\max}$), γ_c are shear strength, reference strain, strain at reverse point, respectively.

The tangent shear modulus can be derived from equation.

$$G_t = \frac{G_{\max}}{\left[1 + \frac{|\gamma - \gamma_c|}{2\gamma_r}\right]^2} \quad \text{for initial loading} \tag{3}$$

$$G_t = \frac{G_{\max}}{\left[1 + \frac{|\gamma|}{2\gamma_r}\right]^2} \quad \text{for reloading and unloading} \tag{4}$$

Since this model is a model with changing elastic modulus, no residual or plastic volume deformation remains after loading. In order to calculate the residual or plastic volume deformation, the foregoing empirical relations between the shear strain and volume strain, Martin and Byrne equations, are incorporated into the hyperbolic model.

In an undrained simulation, a variation of pore pressure is related to a variation of volumetric strain through the formula:

$$\Delta p = -\frac{k_w}{n}\Delta\varepsilon_{ii} \tag{5}$$

where $k_w$is the fluid bulk modulus and n is the medium porosity. In a coupled fluid-mechanical simulation, the incremental elastic stress–strain relations can be expressed:

$$\Delta\sigma_{ij} = 2G\Delta\varepsilon_{ij} \tag{6}$$

$$\frac{1}{3}\Delta\sigma_{ii} = (k + \frac{k_w}{n})\Delta\varepsilon_{ii} \tag{7}$$

The maximum shear modulus was calculated using the following equations

$$G_{\max} = \rho v_s^2 \tag{8}$$

where $\rho$and v_s are mass density and shear wave velocity, respectively.

$$G_{\max} = 1230\mathrm{OCR}^k \frac{(2.973 - e)^2}{1 + e}(\sigma_0')^{0.5} \tag{9}$$

where OCR, σ_0', e, and k are overconsolidation ratio, mean principal effective stress, void ratio, and a factor depending on the plasticity index, respectively.

The bulk modulus is expressed in the following equation:

$$B = (2G_{\max}(1 + v)/(3(1 - 2v) \tag{10}$$

where $G_{\max}$ and v are maximum shear modulus and Poisson's ratio, respectively.The shear strength, $\tau_{\max}$, is computed using

$$\tau_{\max} = 0.5\left(\sigma_1^{'} + \sigma_3^{'}\right)\sin(\phi^{'}) + c\cos(\phi^{'}) \quad (11)$$

where $\sigma_1^{'}$, $\sigma_3^{'}, \phi$, and c are effective maximum principal stress, effective minimum principal stress, friction angle, and cohesion, respectively.

Since the hyperbolic model uses a tangent elastic modulus, no residual or plastic volume deformation remains after the loading. In order to calculate the residual or plastic volume deformation, the empirical Martin et al. (1975) and Byrne (1991) relations between the shear strain (γ) and volumetric strain (ε_{vd}) were incorporated into the hyperbolic model.

$$\Delta\varepsilon_{vd} = C_1(\gamma - C_2\varepsilon_{vd}) + C_3\varepsilon_{vd}^2/(\gamma + C_4\varepsilon_{vd}) \quad (12)$$

where, $\Delta\varepsilon_{vd}$, ε_{vd} and γ are the incremental volumetric strain, accumulated volumetric strain, and the amplitude of the last cycle of shear strain, respectively. C_1, C_2, C_3, and C_4 are empirical constants and $C_1 \cdot C_2 \cdot C_4 = C_3$. The other relation used was the one later proposed by Byrne (1991):

$$\Delta\varepsilon_{vd}/\gamma = C_1\exp\left(-C_2\varepsilon_{vd}/\gamma\right) \quad (13)$$

where $C_1 = (N_1)_{60}^{-1.25}$ and $C_2 = 0.4/C_1$. The shear strain, γ, in the two equations is defined as the peak-to-peak shear strain and $(N_1)_{60}$ is the corrected SPT blow count for 1 tsf overburden and 60% hammer efficiency (blows/ft).

Biot's consolidation theory is applied in FLAC to simulate the dissipation of excess pore water pressure caused by the seismic loading. The modified Hyperbolic/Byrne model was implemented into FLAC as the constitutive relations for the different soil layers used in the embankment simulations.

3 Shaking Table Test

A shake table test was performed in the structures high bay laboratory of Missouri University of Science and Technology in Rolla, MO. To determine the shaking-induced displacement and dynamic response of a model of the A1466 highway embankment and to calibrate the numerical model.

3.1 Physical Modeling Philosophy

This shaking table test was limited to a one dimensional dynamic loading due to the inherent setup of the shaking table and it was conducted in a 1-g environment. The model soil has a similar density to that of the prototype soil. Though the embankment is above the ground water table, the embankment soil is assumed to be saturated to simplify the constitutive scaling requirements, since undrained stress–strain response is independent of confining pressure for saturated clays. Based on dimensional analysis, the scale factors such as time, mass, length, etc., can be expressed in terms of the geometric scaling factor, λ, as shown in Table 1.

A small-scale embankment was constructed and tested in a rigid box container that was bolted to the shake table. The container was made of plywood, as shown in Fig. 1. Its internal dimensions were 0.6 m wide, 1.5 m long and 0.5 m tall. The floor of the container was 3/4 in (2 cm) thick plywood that was secured to the shaking table. To prevent sliding between container base and soil, coarse sand was epoxyed on the surface of the bottom plate. The sides, front, and back of the container were stiffened. Plastic wrap was used to cover the interior sidewalls to minimize friction along the side wall-soil interface. The interior walls were painted to reduce the friction and keep the soil moisture.

3.2 Soil Embankment Prototype Model

Borehole soil sampling, cone penetrometer tests (CPT) and seismic piezocone investigations were conducted at both the top and bottom of the A1466 prototype embankments. The shear wave velocity was measured using a seismic cone penetrometer. A laboratory testing program was conducted to complete the site characterization of the embankment.

Table 1 Scaling relations for primary soil properties (Wartman 1996)

Mass density	1	Acceleration	1	Length	λ
Force	λ^3	Shear wave velocity	$\lambda^{1/2}$	Stress	λ
Stiffness	λ^2	Time	$\lambda^{1/2}$	Strain	1
Modulus	λ	Frequency	$\lambda^{-1/2}$	–	–

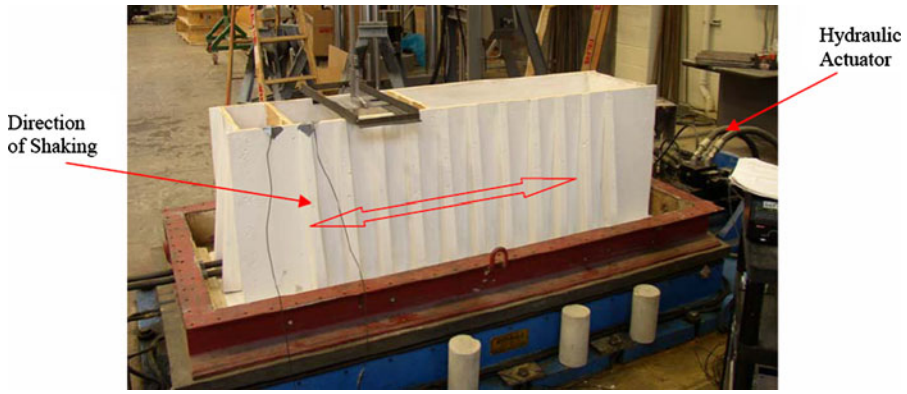

Fig. 1 Stiff plywood container used for shaking table model test

Table 2 Soil properties of embankment at bridge A1466 used for the shaking table test

Soil property	Average value
Unit weight (kN/m^3)	19.85
Water content (%)	24.4
Plasticity index	20
Undrained shear strength (kPa)	10.8
Friction angle (°)	35
Shear wave velocity (m/s)	200
Void ratio	0.66

The embankment soil was classified as low plasticity clay (CL). The soil properties used to model the behavior of this embankment are shown in Table 2.

The nonlinear modulus degradation and damping curves are not directly modeled from the prototype. Therefore, only undrained shear strength and shear modulus can be the principal soil modeling criteria. Soil shear modulus should be properly modeled for elastic analysis and the undrained shear strength should be emphasized for inelastic analysis. Both of these properties are accounted for in a full nonlinear analysis. However, the problem is complicated since they have different scaling factors, λ for undrained shear strength and $\lambda^{1/2}$ for shear wave velocity. Therefore, the "true" model similarity cannot be achieved practically. The feasible method is to model the primary soil properties and ignore the secondary effects to obtain an "adequate" model with the primary features of the problem (Moncarz and Krawinkler 1981). The model soil was directly excavated from the prototype embankment and transported to the laboratory. A 1:1 slope was used for the model embankment since the model soil was stiff and not totally saturated. This slope was chosen to insure that a sufficiently large deformation would occur during shaking. The details on the preparation of shaking table can be found in Liu (2005).

3.3 Measurements and Instrumentation

Two accelerometers were placed at the bottom of the box to check the input motion controller. The input motion applied by the controller was a sine wave at 2.5 Hz frequency. The Fourier amplitude spectra of input motion and the measured acceleration time histories were nearly identical.

The seismic response at three locations was recorded during shaking using accelerometers. Figure 2 shows the response spectra and the Fourier amplitude spectra of the three locations shown in Fig. 3. The Fourier amplitude at accelerometers 3 and 4 are deamplified, and the spectral accelerations were amplified. However, they were very close. The spectral accelerations and Fourier amplitudes at accelerometer 5 were both deamplified. They were very narrow in response spectra and wide in Fourier spectra. The predominant frequency from Fourier spectra was 2.5 Hz for all input and measured motions. The predominant period from response spectra was 0.4 s, as expected from the input motion.

The profiles of the model embankment before and after shaking are shown in Fig. 3a. The maximum horizontal displacement was about 3 mm occurring at the middle of the face of the slope. The maximum vertical displacement of about 3 mm occurred at the top of the slope.

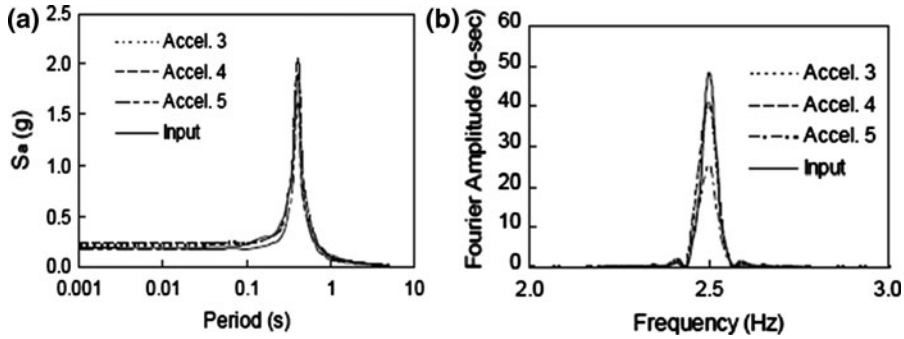

Fig. 2 Model embankment seismic responses on shaking table **a** response spectra; **b** fourier amplitude spectra

4 Calibration of Modified Models

4.1 Calibration Against Shaking Table Test

The shaking table physical model embankment was simulated using FLAC and the modified hyperbolic model. The bottom of the model embankment was fixed, and a beam element was placed at the left side of the model embankment to simulate the plywood box. Both isoparametric, constant-strain triangle and rectangle elements using mixed discretization were generated to calculate the element stiffness matrices. A sine-wave forcing function was the input motion at the bottom of the box. The input motion was simplified to a harmonic sinusoidal wave. A sine wave with a 2.5 Hz frequency and a peak displacement of 0.305 in (8 mm) was used to generate an equivalent acceleration of 0.19 g. This is equal to $0.65a_{max}$. Fifty-one cycles were employed to reach the duration of 20.5 s. The bottom boundary was fixed. Free-field boundaries were applied to the vertical sides of the model to minimize wave reflections and achieve free-field conditions. The soil properties and the model embankment profile were taken from the shaking table tests. A profilometer was used to monitor the embankment profile before and after the shaking. A base was fabricated using two steel angle bars which can move along the top of the mold container. A vernier caliper or steel ruler can be moved up and down vertically to take readings along the slope profile through the steel base. White grease was injected into the embankment through holes drilled along the slope. The grease columns deformed with the embankment during flight. Careful exhumation of the grease columns after flight were meant to measure the deformation inside the embankment. The profilometer was used to measure the deformation of the grease column before and after shaking to find the sliding plane. Accelerometers were placed at several key locations such as top, bottom, and inside the model soil. ThetaShear Type 4507/4508 accelerometers were used. A Datarec-A60 data acquisition system with six channels was used for acceleration time history acquisition. The recording rate is 500 values per second. The response at the instrumented locations were recorded and compared with the measured ones. Figure 4 shows the response spectra for accelerometers No. 4 and 5, which agree very well at the predominant period. At the higher or lower periods, the calculated values were a little bit higher than the measured values, but they are comparable. The calculated final deformation is shown in Fig. 3b,

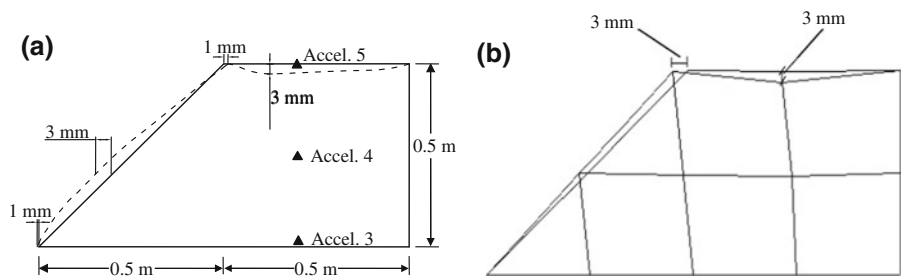

Fig. 3 Deformed embankment profile **a** measured in shaking table test; **b** calculated using the hyperbolic model

which can be compared with the measured deformation. The maximum horizontal deformation was about 3 mm and the maximum vertical deformation was about 3 mm. The magnitude of the calculated deformation agreed with the measured one. The horizontal deformation pattern was different in spite of the similar magnitude, which mainly resulted from the assumed boundary condition. The bottom of the model embankment was fully fixed in the numerical simulation. But a small 1-mm slide may occur in the shake table test. The vertical deformed pattern is almost identical to the measured one, as shown in Fig. 3. All of these indicate that the implemented hyperbolic model is able to capture the main mechanism of the dynamic response and the deformation study of the embankment.

4.2 Calibration Against a Case History

To further verify the modified hyperbolic model's ability to analyze the seismic performance of the embankment, the model was also calibrated against the famous 1971 failure of Upper San Fernando Dam, located in southern California. This hydraulic fill dam was constructed on about 15–18 m of alluvium overlying bedrock. It is about 21 m high. A 5.5-m-high rolled fill section was placed on the upstream portion of the hydraulic fill, leaving a 30.5 m wide bench on the downstream slope. The representative cross section with 2.5H:1V slope is shown in Fig. 5. This dam did not fail during the earthquake. However, post earthquake deformations were measured and, therefore, provided a case study that could be used to calibrate the results of the numerical modeling.

The ground motion most commonly used to evaluate the response of the San Fernando dams to the 1971 San Fernando earthquake was one that was originally developed shortly after the earthquake. It is a modified form of the actual recording from the Pacoima Dam abutment. The report by Seed et al. (1973) has a description of this modified record (EERC 73-2). The PGA is about 0.6 g, the predominant period is 0.4 s and the duration is about 40 s.

SPT tests were performed at the site during April and May 1971, as reported by Harder and Seed (1986). Soil properties for the dynamic analysis are given in Table 3.

The computed deformations using the Finn model and the modified hyperbolic model, as well as the measured displacements (Seed et al. 1973) at different locations at the end of the earthquake are shown in Table 4. The different locations are shown in as a number inscribed by a circle in Fig. 5. The calculated displacements using the Finn model, are lower than the measured values (Seed et al. 1973). This discrepancy could result from the uncertain soil properties and the crude bilinear model itself. The displacements are comparable with the modified measured values (Serff et al. 1976). Overall, the deformed pattern is similar, as shown in Fig. 6. Consequently, the Finn model can provide a predictions of earthquake-induced deformations but not close to the magnitude measured, especially in the x direction (horizontal).

The calculated displacements using the hyperbolic model agree well with the measured values modified by Serff et al. (1976). The deformed pattern is almost the same as that shown in Fig. 6. The measured and modified measured displacements are close only at

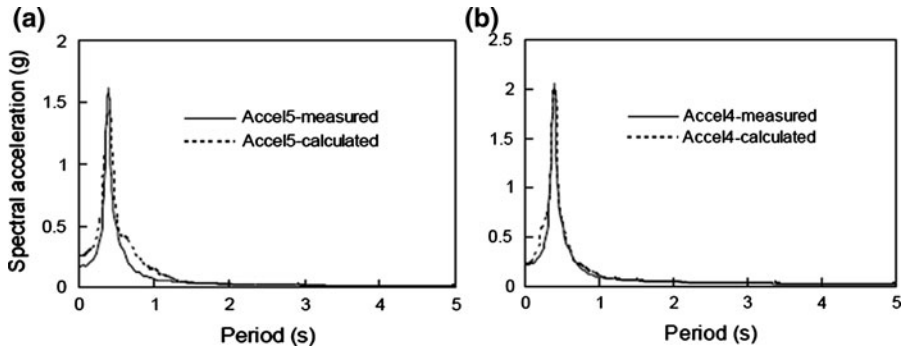

Fig. 4 Comparison of measured and calculated response spectra. **a** at accelerometer No. 5; **b** at accelerometer No. 4

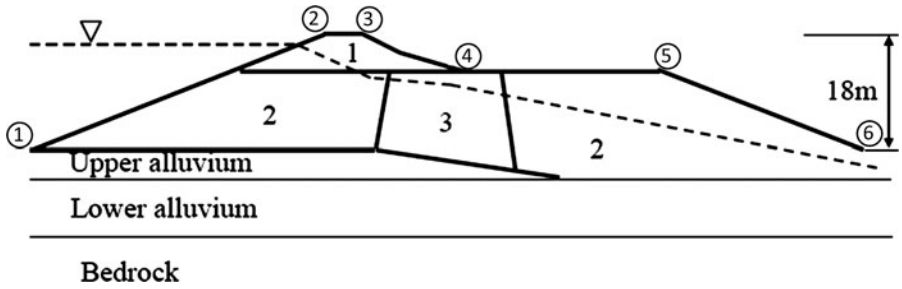

Fig. 5 Soil profile of Upper San Fernando Dam (Seed et al. 1973). *Embankment zones 1* rolled fill, *2* hydraulic fill sand, *3* hydraulic fill clay core; the numbers inscribed in the *circles* are the points investigated in terms of displacements

Table 3 Soil properties for dynamic analysis for San Fernando Dam

Parameter	Unit weight		Strength		Stiffness		
	Moist (kN/m^3)	Saturated (kN/m^3)	c (kPa)	ϕ' (°)	K_{2max}	K_b	m
Hydraulic fill and clay core	18.9	19.2	0	37	30	230	0.26
Rolled fill	21.0	22.0	125	25	30	100	0.38
Alluvium upper/lower	–	20.3	0	37	40/110	150	0.40

m is the confining stress exponent

Table 4 Calculated, measured and modified measured deformations for San Fernando dam

Position	Finn model		Modified hyperbolic model		Measured (Serff et al. 1976)		Measured (Seed et al. 1973)	
	x (m)	y (m)	x (m)	y (m)	x (m)	y (m)	x (m)	y (m)
Point 1	−0.61	0.05	0.66	0.11	–	–	–	–
Point 2	0.11	−0.47	1.28	−0.65	1.49	−0.76	1.52	−0.91
Point 3	0.23	−0.37	1.34	−0.85	–	–	–	–
Point 4	0.57	−0.11	1.60	−0.06	1.95	−0.06	–	–
Point 5	1.59	−0.90	1.34	−0.05	2.2	−0.43	–	–
Point 6	0.63	0.19	1.45	−0.03	1.1	−0.06	–	0.61

point 2 and totally different at point 6. The reason may be that the modified measured values are inferred from the numerical and empirical analysis. Compared with the original measured values, the hyperbolic model can give very good results. Therefore, the hyperbolic model appears to provide reasonable results and better understanding of the deformation of earth structures during earthquakes.

5 Application of the Modeling Technique to NMSZ Highway Embankments

The calibrated hyperbolic model was applied to determine the deformations in the transverse cross section of the approach embankment to Bridge A1466 in the NMSZ. To reduce the boundary effects, the depth of 37 m of foundation soils was included in the embankment system, as shown in Fig. 7. Ground motions were input at the bottom of the model. Ground motions were obtained from the site response analysis accounting for high confining pressure effect (Liu 2005). A total of five horizontal ground motions at M7.0 normal to the longitudinal axis of the bridge were used for this study to understand the general behavior of the embankment-foundation soil system. The duration of ground motions was 82 s. The fundamental period ranges from 0.3 to 0.5 s and the spectral accelerations range from 0.5 to 0.8 g. Index, permeability, and triaxial tests were conducted on the

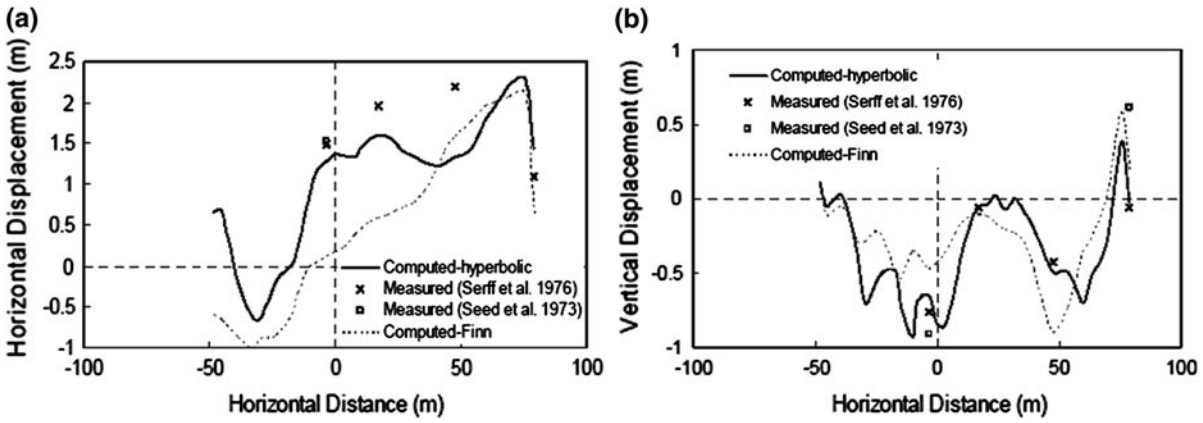

Fig. 6 Displacements along embankment profile **a** horizontal displacement; **b** vertical displacement

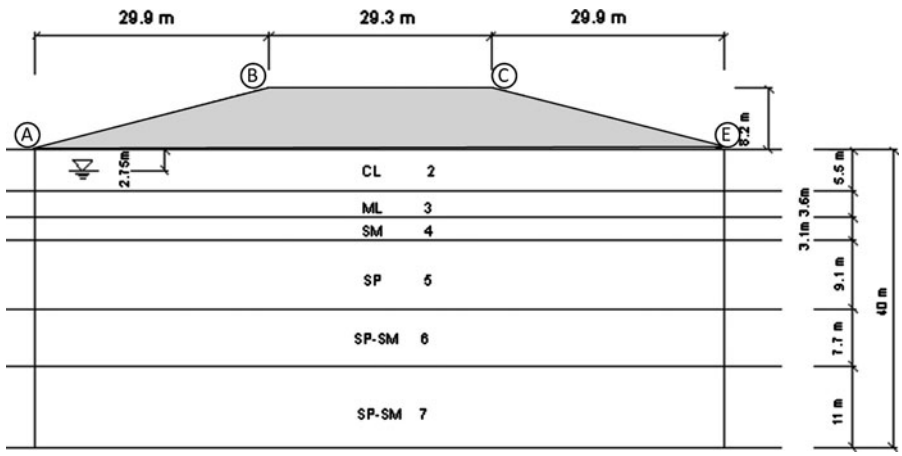

Fig. 7 Embankment profile including foundation soils regarding the A1466 bridge in the NMSZ (Missouri). *A*, *B*, *C*, and *D* are the points investigated in terms of displacements

samples taken from the embankment and foundation soils. The soil parameters of the embankment and foundation soils are shown in Table 5.

The horizontal and vertical displacements along the embankment surface are calculated based on the hyperbolic model and shown in Fig. 8. The locations of points are shown in Fig. 7. Figure 8 shows the horizontal and vertical displacements along the embankment surface for different magnitudes of ground motion normal to the approach embankment

Table 5 Soil parameters of the embankment and foundation soils regarding the bridge A1466 in NMSZ (Missouri)

Soil unit	Soil material	Density (Mg/m^3)	c′ (kPa)	ϕ' (°)	Shear modulus, G (kPa)	Porosity, *n*	$(N_1)_{60}$
1	CL	2.023	10.8	35	59,848	0.4	19
2	CL	1.947	34.5	30	44,393	0.44	11
3	ML	1.876	0	32	56,136	0.48	9
4	SM	2.161	0	31	89,935	0.3	8
5	SP	2.181	0	45	118,429	0.28	40
6	SP-SM	2.120	0	44	112,163	0.32	36
7	SP-SM	1.916	0	44	179,445	0.44	36

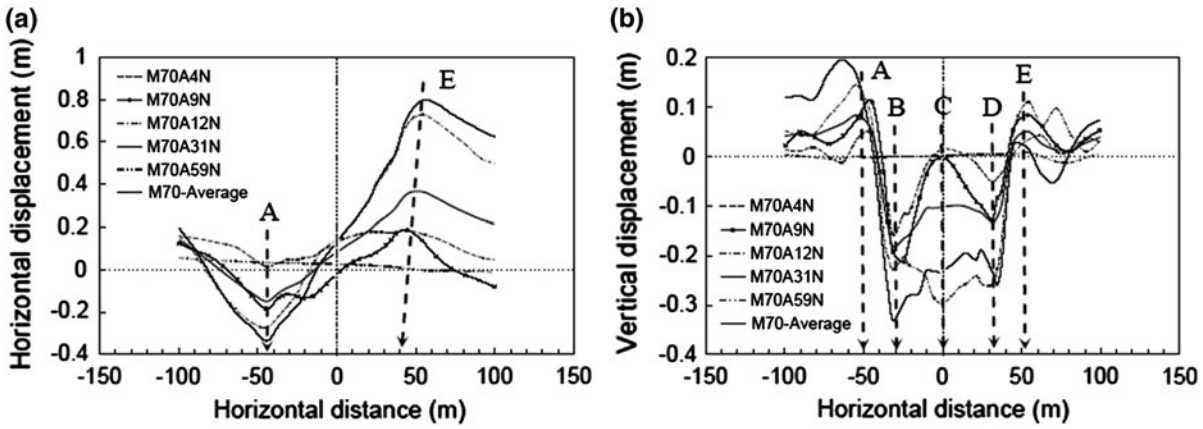

Fig. 8 Displacement along surface of the approach embankment to bridge a1466 **a** horizontal displacement; **b** vertical displacement

alignment. Several acceleration time histories developed from a M7.0 earthquake simulation were applied to the modeled embankment. The maximum horizontal displacements in the positive *x*-direction occurred at location *E*, and in the negative direction they occurred at location *A*. The maximum horizontal displacements in the positive *x*-direction range from 0 to 0.8 m. The maximum negative horizontal displacement is −0.35 m. The minimum horizontal displacements occurred at point A ranging from 0.1 to 0.4 m. The vertical displacements are symmetrical along the middle of the embankment. The maximum settlements occurred at locations B and D, ranging from 0.15 to 0.35 m. Heave happened in front of the toe. It can be observed that the slope slide along a surface and maximum deformation occurred near the toe of the slope.

6 Conclusion

The modified hyperbolic model was implemented into FLAC and calibrated against a shaking table test and the 1971 failure of the upper San Fernando Dam. The modified hyperbolic model is able to match better both the laboratory model and the case study, when compared to the Finn model included with the FLAC program. The shaking table test was performed by doing a small-scale embankment with the principle of similitude. The results of the two simulation using modified hyperbolic model indicate that it can provide a good estimate for the earthquake-induced deformation. Then the model was applied to study the permanent deformation of the bridge approach embankment at Bridge Site A1466 in the NMSZ. It is predicted that the embankment would experience a large deformation in the embankment during an earthquake with a magnitude larger than M7.0. The maximum horizontal displacements take place at the toe of the embankment (up to 0.8 m), and heave occurs in front of the toe of embankment (up to 0.2 m).

References

Byrne PM (1991) A cyclic shear volume—coupling and porewater pressure model for sand. Second international conference on recent advances in geotechnical earthquake engineering and soil dynamics, St. Louis, Missouri, Report 1.24, vol 1, pp 47–56

Finn WDL, Yogendrakumar M, Yoshida N (1986) TARA-3: a program to compute the response of 2-D embankment and soil-structure interaction systems to seismic loadings. Department of Civil Engineering, University of British Columbia, Vancouver

Finn WDL, Sasaji Y, Wu G, Thavaraj T (1999) Stability of flood protection dikes with potentially liquefiable foundations: analysis and screening criterion. In: Proceedings of 13th annual vancouver geotechnical society symposium, Vancouver pp 47–54

Harder LF, Seed HB (1986) Determination of penetration resistance for coarse-grained soils using the becker hammer drill. Report UCB/EERC-86/06, Earthquake Engineering Research Center, University of California, Berkeley

Lin J-S, Hynes M-E (1998) Seismic discontinuous deformation analysis. In: Proceedings of the geotechnical earthquake engineering and soil dynamics III, Seattle, WA, pp 790–799

Liu WX (2005) Seismic site response of deep soil and embankments in the new madrid seismic zone. Ph.D. thesis, University of Missouri-Rolla

Makdisi FI, Seed HB (1978) Simplified procedure for estimation dam and embankment earthquake-induced deformations. J Geotech Eng Div ASCE 104:849–867

Martin GR, Finn WDL, Seed HB (1975) Fundamentals of liquefaction under cyclic loading. J Geotechn Eng Div ASCE 101(GT5):423–438

Masing G (1926) Eigenshannungen Und Verestigung Beim Messing. In: Proceedings of the second international congress of applied mechanics

Moncarz P, Krawinkler H (1981) Theory and application of experimental model analysis in earthquake engineering. Rpt No 50, John Blume Earthquake Eng Ctr, Stanford University

Muraleetharan KK, Mish KD, Yogachandran C, Arulanandan K (1988) DYSAC2: dynamic soil analysis code for 2-dimensional problems, Department of Civil Engineering, University of California, Davis, California

Newmark N (1965) Effects of earthquakes on dams and embankments. Geotechnique 15(2):139–160

Prevost JH (1981) DYNAFLOW: a nonlinear transient finite element analysis program. Department of Civil Engineering, Princeton University, Princeton, NJ

Rathje EM, Bray JD (1999) An examination of simplified earthquake-induced displacement procedures for earth structures. Can Geotech J 36(1):72–87

Seed HB, Lee KL, Idriss IM, Makdisi F (1973) Analysis of the slides in the San Fernando dams during the earthquake of February 9, 1971. Report No. EERC 73–2. University of California, Berkeley

Serff N, Seed HB, Makdisi FI, Chang CY (1976) Earthquake induced deformation of earth dams. UCB/EERC-76/04, Earthquake Engineering Research Center, University of California, Berkeley

Wartman J (1996) The effect of fly ash on the geotechnical properties of a soft clay. M. Eng. Thesis, University of California, Berkeley

Wu G (2001) Earthquake-induced deformation analysis of the upper San Fernando Dam under the 1971 San Fernando earthquake. Can Geotech J 38(1):1–15

Wu G (1998) VERSAT: a computer program for static and dynamic 2-dimensional finite element analysis of continua, release 98, Wutec Geotechnical International, Vancouver

Zienkiewicz OC, Chan AHC, Pastor M, Paul DK, Shiomi T (1990a) Static and dynamic behavior of soils: a rational approach to quantitative solutions. Part I: fully saturated problems. Proc R Soc Lond Ser A 429:285–309

Zienkiewicz OC, Xie YM, Schrefler BA, Ledesma A, Bicanic N (1990b) Static and dynamic behavior of soils: A rational approach to quantitative solutions. Part II: semi-saturated problems. Proc R Soc Lond Ser A 429:311–321